

Computer-aided Formal Proofs about Dendritic Integration within a Neuron

Ophélie Guinaudeau¹, Gilles Bernot¹, Alexandre Muzy¹, Daniel Gaffé² and Franck Grammont³

¹Université Côte d'azur, CNRS, I3S, France

²Université Côte d'azur, CNRS, LEAT, France

³Université Côte d'azur, CNRS, LJAD, France

Keywords: Single Neuron Modelling, Dendrites, Signal Integration, Formal Methods, Model Checking.

Abstract: This article is threefold: (i) we define the first *formal* framework able to model dendritic integration within biological neurons, (ii) we show how we can turn continuous time into discrete time consistently and (iii) we show how a Lustre model checker can automatically perform proofs about neuron input/output behaviours owing to our framework.

Our innovative formal framework is a carefully defined trade-off between abstraction and biological relevance in order to facilitate proofs. This framework is *hybrid*: inputs entering the synapses as well as the soma output are discrete signals made of spikes but, inside the dendrites, we combine signals quantitatively using real numbers. The soma potential is inevitably specified as a differential equation to keep a biologically accurate modelling of signal accumulation. This prevents from performing simple formal proofs. This has been our motivation to discretize time. Owing to this discretization, we are able to encode our neuron models in Lustre. Lustre is a particularly well suited flow-based language for our purpose. We also encode in Lustre a property of input/output equivalence between neurons in such a way that the model checker Kind2 is able to automatically handle the proof.

1 INTRODUCTION

Many studies suggest that there is a strong interdependence between morphology and information processing capabilities of a neuron (Bianchi et al., 2012; Mohan et al., 2015; Hu and Vervaeke, 2017). In this pioneering work, we make use of *formal methods* from computer science to investigate how single neurons process information, with a particular emphasis on their dendritic morphology.

Neurons are the building blocks of the brain. They are highly connected and communicate through electrical impulses. Typically, neurons receive those signals on branched extensions called *dendrites*, at specific locations named *synapses* (Figure 1). All the stimuli are finally integrated at the *soma*. If the resulting signal accumulation is strong enough, it is transmitted to neighbouring neurons through the *axon* which is another kind of extension. There are many types of neurons (Mel, 1994; Stuart et al., 2016) and some of them are structurally and functionally very different from the standard one described above, depending on the respective sizes on the constituting

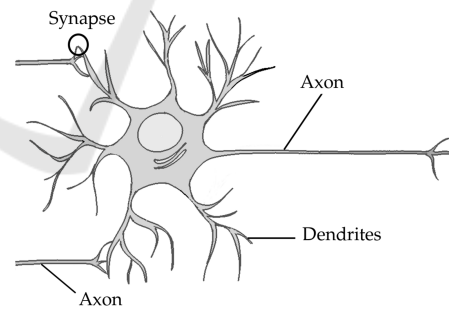


Figure 1: Schematic representation of a standard biological neuron.

sub-parts.

There can be between a few to several tens thousands of synapses as a result of the connectivity level of the neuron. The incoming signals interact continually in time and space and while propagating through the dendrites towards the soma, signals are significantly modified. Indeed, many parameters of information-processing such as signal filtering, response speed and connectivity, are strongly influenced by the dendrites properties (Williams and Stu-

art, 2002; Stuart et al., 2016). Therefore, it makes this sophisticated structure a key determinant of neuronal computation.

A combination of experimental and theoretical work is required to make the link between structure and function of neurons. Nowadays and despite recent advances, dendrites are still difficult to study experimentally mainly because of their small size. Theoretical modelling frameworks are thus helpful to overcome these limitations as they provide a rigorous support for understanding how such complex behaviours emerge. Since Rall's pioneering work, some theoretical models have been dedicated to dendrites structure and physiology (see Section 2). However, these models mainly focus on microscopic biophysical aspects of dendrites physiology, making difficult the scaling from a computational point of view. On the other side, most models focusing on this computational efficiency neglect dendritic morphology and integration properties.

Our goal is to use formal methods from computer science to prove properties on complete neurons and allow automated identification of parameters, at the cost of a minimal set of simplifying assumptions. We define here a model of neuron sufficiently simple to use formal methods while taking into account the dendritic structure. Basically, we propose a relevant trade-off between abstraction and biological relevance. This model is hybrid as its inputs and output are discrete while we consider linear equations on real numbers within the neuron.

The next section presents some relevant existing single neuron models. In Section 3, we introduce our model with mathematical definitions of its components and its dynamics. We then explain in Section 4, how to discretize time in order to prove some properties on neurons using model checking.

2 STATE OF THE ART

Numerous single neuron models are found in the literature. Depending on the research objectives, they can be classified on a variety of criteria: computational or biophysical, discrete or continuous, punctual or structural, with rate coding or temporal coding, *etc.*

The purpose of this section is not to give the huge exhaustive list of existing models, it rather aims at positioning our work with respect to some of them.

Computational Versus Biophysical Models. Opposing computational to biophysical models is a classic way to characterize single neuron models (Brette, 2003). In the case of computational models, neurons are highly abstract in order to facilitate the study of

global behaviours under certain hypotheses. A good example to illustrate this type of models, is the formal neuron of McCulloch and Pitts (M&P) (McCulloch and Pitts, 1943). It has multiple inputs (by analogy with synapses in biological neuron) and a unique output (which can be compared to the axon). The output is a binary variable which is calculated as a function of the weighted sum of the inputs. If the sum exceeds a given threshold, the neuron becomes active (its state is equal to 1), otherwise, it becomes inactive (its state is equal to 0). Despite its apparent simplicity, this model is remarkably powerful as such neuron networks allow to implement any calculable function. However, this kind of very simple models is of low interest for a biological understanding of the neuronal functioning.

On the contrary, biophysical models aim at representing in details the physico-chemical mechanisms driving biological functions. The most famous and widely used biophysical model is perhaps Hodgkin and Huxley's (H&H) (Hodgkin and Huxley, 1952). It describes the action potential generation at the axon hillock, based on ionic channels dynamics.

Our work, is a trade-off between those two types of models. We are more interested in how the neuron "computes" to relate input signals to an output, rather than in the precise biochemical mechanisms involved in this input/output function. Nevertheless, most of our definitions are sensible abstractions of biophysical processes (Section 3).

Discrete Versus Continuous Models. M&P's neuron is a typical discrete model as the values are discrete (either 0 or 1) and the time is discrete too (the state of the neuron is calculated at each step).

On the contrary, H&H's model is continuous as it is governed by a set of differential equations. Most of the biophysical models are, by nature, continuous. It is worth mentioning another well-known continuous model: the Integrate-and-Fire (I&F) model (Lapicque, 1907; Brunel and Van Rossum, 2007). It represents the membrane as an electrical circuit and describes the electrical potential of the neuron with a differential equation. There are many extensions of this model including the Leaky I&F, quadratic and exponential versions (Brette and Gerstner, 2005; Börgers, 2017).

Our work is a hybrid formalism. Unlike the I&F model which does not explicitly represent the electrical impulses, we focus on them: the sequence of impulses actually constitutes the input/output of our neuron. This input/output is thus discrete while the electrical potential of our neuron is continuous (see Section 3). We share similarities with the work of Maass (Maass, 1999; Maass, 1996), as signals ex-

changed by neurons are discrete. Moreover, modelling of synapses uses piecewise linear functions. However, Maass does not focus on dendritic integration and is rather interested in networks.

Punctual Versus Structural Models. As already mentioned, punctual models represent a neuron as a “point,” totally ignoring its morphology. Most of single neuron models are punctual including all the previously discussed ones. In some studies, artificial delays are added to neurons in order to compensate the lack of morphology (Izhikevich, 2006).

Some models focus on the neuron structure. This is the purpose of Cable Theory (CT) which was first used to describe the propagation of electrical signals through submarine cables. It was then applied to neurons in the 1960’s by Rall, a pioneer of dendrites modelling. Dendrites are seen as cylinders in which signal propagates following a second order partial differential equation with dendrites physico-chemical properties as parameters (Rall, 1959; Rall, 1962). This equation has been solved analytically for some particular conditions and it is widely used as part of simulators such as GENESIS (Bower, 2003).

All in all, punctual models facilitate the use of formal methods. However, they do not allow the study of dendritic integration.

Rate Coding Versus Temporal Coding Models. A classic point of view is that activity of neurons is encoded by their firing frequency. This rate coding has been long at the basis of many neuron models. As a simple example, there are second generation neurons which are similar to M&P’s neuron but with a continuous activation function instead of a threshold gate. Their output is a sequence of real numbers which can be seen as an instantaneous frequency. It implies that the exact times of firing are not taken into account, thus ignoring synchronization phenomena experimentally observed in the brain (Brette, 2003). However, temporal coding is of growing interest. With this approach, the most important variable is the electrical impulse per se and not the frequency. The I&F is one of the most widely used model of this type.

In this paper, we are interested in the role of the dendrites in the neuronal function. Therefore, we need a non punctual model. Moreover, our goal is to use formal methods to prove properties on neurons. As a matter of fact, the larger the number of parameters, the harder the model validation (Popper, 1963), especially with computer-aided proofs. Purely biophysical models are thus not suitable for our purpose. We decided to define a new framework dedicated to our formal study, and we decided to adopt the temporal coding paradigm. This framework is described in the

following section along with the biological foundations and the hypotheses we made.

3 HYBRID FORMAL NEURON MODEL

A *tree* being defined as a root node to which are recursively attached children trees, our single neuron model can be defined as dendritic trees connected to a root soma (denoted ∇) (Figure 2). In our model, we ignore the axon as, in first approximation, it transmits the signal faithfully. Dendrites are divided into *compartments*, each one being delimited by either *branching points* or *synapses*. A formal neuron is thus a forest of dendritic trees composed of formal synapses (leafs) and compartments (branches) linked together at branching points. Each tree of the forest is rooted on ∇ . The following subsections give the formal definitions and the dynamics of these basic components.

We note \mathcal{N} the set of all neurons and, given a neuron N , we note $Sy(N)$ the set of its synapses and $Co(N)$ the set of its compartments.

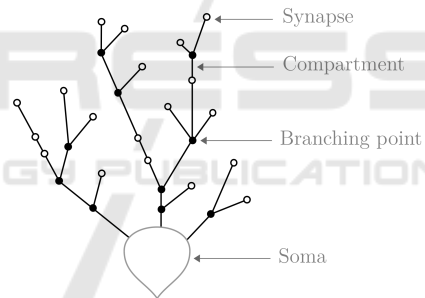


Figure 2: Schematic representation of our single neuron model.

We can see the neuron as a system which receives discrete inputs at synapses, converts them into a continuous signal and re-discretizes it in the soma. Electrical signals processed by neurons are basically ionic charge flows along the tree, making the potential locally changing. From our formal point of view, we consider an abstract notion of charges/potential using real numbers.

3.1 Synapses and Input Signal

Synapses are the input ports of neurons, the locations where they receive electrical signals coming from other neurons. In the brain, signals are sequences of electrical impulses called action potentials or *spikes*. When a spike (sent by another neuron) reaches a synapse, it triggers a local variation of the neuron

electrical potential. This effect, called post-synaptic potential (PSP), is due to ionic movements through the membrane. Depending on the synapse, the PSP can be either excitatory or inhibitory, respectively increasing or decreasing the potential.

In our modelling, we focus on spike times. An input signal (ω) is a function of time which is equal to 1 at spike times and 0 otherwise. Each spike is converted by the synapse into a continuous *trace* comparable to a PSP. For each synapse s receiving a spike, the trace reaches a maximum absolute value (v_s) after a certain delay ($\hat{\tau}_s$) and take a certain time ($\check{\tau}_s$) before being back to the resting value (zero here, see Figure 3). Even though it is described as exponential by biophysical models (Rall, 1959; Rall, 1962; Rall, 1967), we assume that this potential perturbation is linear. This approximation is justified by experimental observations showing that the kinetics do not strictly follow theory (Koch, 2004). As mentioned before, piecewise linear functions were also used in (Maass, 1999) to represent PSPs.

The potential increase triggered by one spike is most of the time not sufficient for the neuron to reach its threshold and transmit the signal. The PSPs are added if the spikes received at a synapse are separated by a sufficiently small time interval: it is called *temporal summation*. We reproduce this phenomenon by summing the traces (Figure 3).

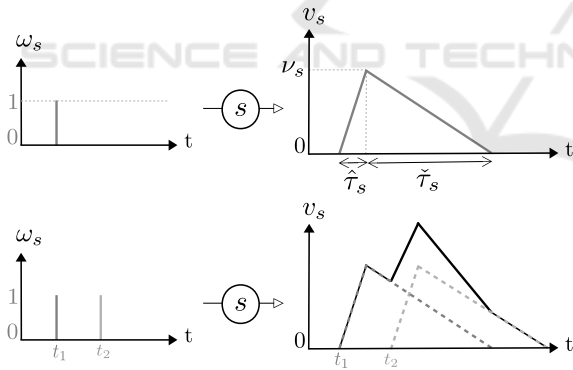


Figure 3: Trace of signals on a synapse s .

Formal definitions are given below.

Definition 1. [Synapse] A synapse s is a tuple $(v_s, \hat{\tau}_s, \check{\tau}_s)$ where v_s is a non-zero real number called maximal potential of a spike for s . If $v_s > 0$ then s is said excitatory, otherwise it is said inhibitory. $\hat{\tau}_s$ and $\check{\tau}_s$ are strictly positive real numbers respectively called rise time and descent delay of the potential.

Definition 2. [Signal] A signal is a function $\omega : \mathbb{R}^+ \rightarrow \{0, 1\}$ such that: $\exists r \in \mathbb{R}^{*+}, \forall h \in \mathbb{R}^+, (\omega(h) = 1 \Rightarrow (\forall h' \in]h, h+r[, \omega(h') = 0))$. The carrier of ω is defined by: $Car(\omega) = \{h \in \mathbb{R}^+ | \omega(h) = 1\}$. Moreover:

- A signal such that $Car(\omega)$ is a singleton $\{u\}$ is called a spike at the time u , noted ω^u .
- Given a neuron N , an input signal for N is a family of signals $\mathcal{S} = \{\omega_s\}_{s \in Sy(N)}$ indexed by the synapse identifiers of $Sy(N)$.

Remark: Obviously, a signal ω can be split into a sum of spikes at times separated by at least r : $\omega = \sum_{u \in Car(\omega)} \omega^u$.

The ultimate goal of the following mathematical construction is to build a signal ω_{∇} called *output signal*, given an initial state and an input signal \mathcal{S} .

Definition 3. [Trace of a signal] The trace of a spike ω^u on a synapse s is the function v_{s, ω^u} defined by:

- If $h \leq u$ then $v_{s, \omega^u}(h) = 0$;
- If $u \leq h \leq u + \hat{\tau}_s$ then $v_{s, \omega^u}(h) = \frac{v_s}{\hat{\tau}_s}(h - u)$;
- If $u + \hat{\tau}_s \leq h \leq u + \hat{\tau}_s + \check{\tau}_s$ then $v_{s, \omega^u}(h) = \frac{v_s}{\check{\tau}_s}(u + \hat{\tau}_s + \check{\tau}_s - h)$;
- If $u + \hat{\tau}_s + \check{\tau}_s \leq h$ then $v_{s, \omega^u}(h) = 0$

Given an input signal ω_s on a synapse s , the trace of ω_s is defined by the real function $v_{s, \omega_s} = \sum_{u \in Car(\omega_s)} v_{s, \omega^u}$.

This definition simply encodes Figure 3.

3.2 Compartments

So far, synapses convert discrete inputs into continuous signals. Those signals then spread through the dendrites. In this work, we only consider propagations towards the soma even though it is known that there exist back-propagation mechanisms (from soma to dendritic tips) (Häusser et al., 2000; Remme et al., 2010). It is also important to note that we do not take into account active properties of the dendrites even though it is clear that dendritic voltage-gated channels play a considerable role in their function (Cook and Johnston, 1997; Johnston and Narayanan, 2008; Stuart et al., 2016). In particular, we do not consider dendritic spikes (Sun et al., 2014; Stuart and Spruston, 2015; Manita et al., 2017). Therefore, this work is under the hypothesis of fully passive dendrites: It is currently the price to pay in order to be able to apply formal methods at this stage.

In passive dendrites, signals are attenuated while spreading. Basically, the flow of ionic charges undergoes a leak because of channels embedded in the neuronal membrane (Figure 4). For biophysical reasons, the more the potential is different between the extracellular media and the inside of the neuron, the more the attenuation is: biological systems usually tend to return to equilibrium. It was well described by CT

model but with the main disadvantage of involving many parameters (Section 2). In our model, we divide the dendrites into small homogeneous compartments. Inspired by the biophysical theory, we characterise compartments using only two parameters: the time for crossing it (δ) and the attenuation applied in a non linear manner to the signal ($\alpha < 1$). At the end of a compartment, the signal is thus multiplied by the α factor after a time δ (Figure 4). We consider a constant throughput whatever the value of the signal. The two parameters α and δ are specific to a given compartment. Concretely they are related to its length, diameter and membrane properties such as resistance and capacitance. Intuitively, the parameters α and δ are a convenient way to hide possibly very sophisticated processes. It constitutes a valuable compromise between biophysical precision and preservation of the ability to perform formal proofs. Also, biophysics suggests that $\hat{\tau}$ and $\check{\tau}$ are elongated within a compartment (Rall, 2011). Here, for the sake of simplicity, we include the total distortion directly in the synapse parameters as we know the synapse locations.

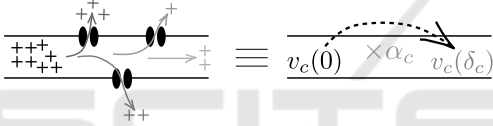


Figure 4: Schematic representation of a compartment from biophysical (left) and computational (right) points of view.

Definition 4. [Compartment] A compartment is a couple $c = (\delta_c, \alpha_c)$ where δ_c is a real number greater or equal to zero and α_c is a real number such that $\alpha_c \in]0, 1]$. If $\delta_c = 0$, then $\alpha_c = 1$.

Additional definitions given below introduce terms and concepts used further.

Terminology 1. Given a neuron N and a compartment $y \xrightarrow{c} z$, y and z are respectively called the input node and output node of c . Moreover, c is called the input compartment of z and we note $In(z)$ the set of input compartments of z .

A predecessor of $y \xrightarrow{c} z$ is a compartment in N of the form $x \xrightarrow{c'} y$ and we note $Pred(c)$ the set of the predecessors of c .

Definition 5. [Contributors] Let N be a neuron. The family $CCo(c)$ indexed by $c \in Co(N)$ is defined inductively as follows:

- $\forall c \in Co(N), \forall c' \in Pred(c)$, if $\delta_{c'} \neq 0$ then $c' \in CCo(c)$;
- $\forall c \in Co(N), \forall c' \in Pred(c)$, if $\delta_{c'} = 0$ then $CCo(c') \subset CCo(c)$.

$CCo(c)$ is called the set of contributor compartments of c . Moreover, the family of sets $CSy(c)$ indexed by $c \in Co(N)$ is defined inductively as follows:

- $\forall c \in Co(N)$, if the input node of c is a synapse s , then s belongs to $CSy(c)$;
- $\forall c \in Co(N)$ and $\forall c' \in Pred(c)$, such that $\delta_{c'} = 0$ then $CSy(c') \subset CSy(c)$.

$CSy(c)$ is called the set of synaptic contributors of c ,

3.3 Soma

The soma (or cell body) of the neuron integrates all the charges coming from the dendrites. When the resulting potential reaches a given threshold, a spike is generated at the axon hillock and transmitted to other neurons. From that time, the neuron enters an *absolute refractory period* (ARP) during which it cannot emit any spike even if its potential is over the threshold. This is due to ionic channels which are inactivated and cannot generate any electrical impulse. Then, the neuron is subject to a *relative refractory period* (RRP) during which a greater signal than usual is needed to trigger a spike.

We model the ARP with an infinite threshold making it unreachable, as it was done in (Maass, 1999). The RRP is represented by an abnormally high threshold ($\theta + \hat{\theta}$), progressively returning to its normal value (θ). Moreover, as in dendrites, there is a leak (γ) at the soma:

Definition 6. [Soma] A soma is a tuple $\nabla = (\theta, \hat{\theta}, \rho, \hat{\rho}, \gamma)$ where θ is the normal threshold, $\hat{\theta}$ is the threshold augmentation, ρ is the duration of the absolute refractory period, $\hat{\rho}$ is the duration of the relative refractory period and γ is the leak. They are all strictly positive real numbers.

To be able to compute when the neuron fires, one needs to know the value of the soma potential (p) at each time. Moreover, because of refractory periods, one needs to know the time elapsed since the last emitted spike (denoted e). The couple (e, p) cannot reach all values because for some values, it would have been necessary to produce a spike before reaching them (thus reinitializing e and subtracting θ from p). We call *nominal* values the possible values for the couple (e, p) (Figure 5).

Definition 7. [Nominal] Given a soma $\nabla = (\theta, \hat{\theta}, \rho, \hat{\rho}, \gamma)$, a couple (e, p) where $e \in \mathbb{R}^+$ and $p \in \mathbb{R}$, is said nominal if $(e < \rho)$ or $(p < \theta)$ or $(p < \theta + \frac{\hat{\theta}(\rho - e)}{\hat{\rho}})$. We note $Nominal(\nabla)$ the set of all the nominal couples.

The state of the soma is the value of the couple (e, p) at a given time (see Definition 8). Thanks to the nominal concept, we were able to formalize soma

dynamics, meaning how p changes in time. This is well defined in Definition 10 with Lemma 1 as a basis. The expression of the derivative is compatible with the Leaky I&F model.

Lemma 1. [Technical lemma]

Given a soma $\nabla = (\theta, \hat{\theta}, \rho, \hat{\rho}, \gamma)$, there exists a unique family of functions $P_F : \text{Nominal}(\nabla) \times \mathbb{R}^+ \rightarrow \mathbb{R}$ indexed by the set of continuous and lipschitzian functions $F : \mathbb{R}^+ \rightarrow \mathbb{R}$, such that for any couple $(e_0, p_0) \in \text{Nominal}(\nabla)$, P_F satisfies:

- $P_F(e_0, p_0, 0) = p_0$
- $\forall h \in \mathbb{R}^+$ the right derivative $\frac{dP_F(e_0, p_0, h)}{dh}$ exists and is equal to $F(h) - \gamma \cdot P_F(e_0, p_0, h)$
- $\forall h \in \mathbb{R}^{+*}$, $\ell = \lim_{t \rightarrow h^-} (P_F(e_0, p_0, t))$ exists and:
 - if $(h + e_0, \ell) \in \text{Nominal}(\nabla)$ then $P_F(e_0, p_0, h)$ is differentiable, therefore $P_F(e_0, p_0, h) = \ell$,
 - otherwise, for any $t \geq h$, $P_F(e_0, p_0, t) = P_G(0, \ell - \theta, t - h)$ where G is defined by: $\forall u \in \mathbb{R}^+$, $G(u) = F(u + h)$.

In other words (Figure 5), from an initial condition (e_0, p_0) , the potential changes following its derivative. It depends on signals coming from the dendrites (F), while taking into account the leak (γ). Every time the potential reaches the threshold, its value is updated (by subtracting θ) and e is reset to zero (keeping the couple (e, p) nominal). Then, the potential follows again its derivative with the new couple (e, p) as initial condition.

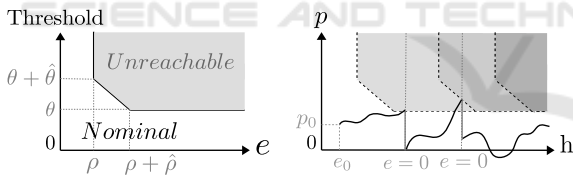


Figure 5: Nominal (e, p) couples and soma dynamics.

3.4 State of a Neuron and Dendrites Dynamics

Intuitively, the state of a neuron is the potential value at each point. So that it is not only the state of the soma (e, p) but also the state of the dendrites (denoted V in Definition 8). According to our compartment definition, we only observe the value of the potential at the beginning and at the end of a compartment (by applying the attenuation factor α). Accordingly, we define the state of a compartment c at a time t as the value of the potential at the end of c between time t and time $t + \delta_c$. Given α_c , δ_c being the time needed for crossing c , it is thus possible to find the potential value at any point of c by “looking into the future” (Figure 6).

Definition 8. [State of a neuron] The state of a neuron N is a triplet $\eta = (V, e, p)$ where:

- V is called the dendritic state of the neuron. V is a family of functions, indexed by $\text{Co}(N)$, the set of the compartments of N ; each function is of the form $v_c : [0, \delta_c] \rightarrow \mathbb{R}$ where δ_c is the crossing delay of the compartment c .
- $e \in \mathbb{R}^+$ represents the elapsed time since the last spike and $p \in \mathbb{R}$ is called the soma potential.

and such that the two following conditions are satisfied:

- for each compartment c :

$$v_c(\delta_c) \sim \left(\sum_{c' \in \text{CCo}(c)} v_{c'}(0) \right) \alpha_c$$

where by convention the comparator “ \sim ” is “ $=$ ” if the input node of c is a branching point, “ \geq ” if its input node is an excitatory synapse, “ \leq ” if its input node is an inhibitory synapse.

- the couple (e, p) is nominal for the soma of N .

We note ζ_N the set of all possible states of the neuron N .

From the state of a neuron, it is possible to define its dynamics (see Definition 10). Soma dynamics is mainly governed by its derivative as seen before. For dendrites, because signals spread unidirectionally through compartments and then from one compartment to another, it is possible to calculate the succession of states by *shifting* as shown in Figure 6 (see Definition 9 and Theorem 1). As a simple example, the potential at the end of a compartment c at a time $h + \delta_c$, is equal to the potential at the beginning of c at time h attenuated by α_c . The potential at the beginning of c at time h is itself equal to the sum of the potentials at the end of its contributors compartments at this given time.

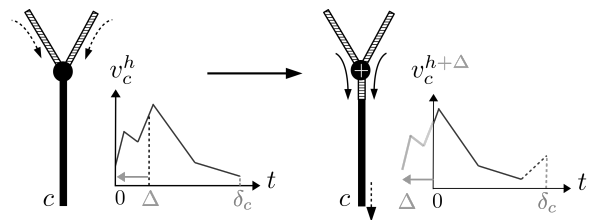


Figure 6: State of a compartment and Δ -shift (Definition 9).

Definition 9. [Δ -shift] Given a neuron N and an input signal $\mathcal{S} = \{\omega_s\}_{s \in \text{Sy}(N)}$, let $V^h = \{v_c^h\}_{c \in \text{Co}(N)}$ be a dendritic state of N at time h and let $\Delta \in \mathbb{R}$ such that $0 \leq \Delta \leq \inf(\{\delta_c \mid c \in \text{CCo}(c)\})$. For any compartment $c \in \text{Co}(N)$, the Δ -shift of v_c^h (noted $\Delta\text{-shift}(v_c^h, \mathcal{S})$), is the function $v : [0, \delta_c] \rightarrow \mathbb{R}$ such that:

- $\forall t \in [0, \delta_c - \Delta], v(t) = v_c^h(t + \Delta);$
- $\forall t \in [\delta_c - \Delta, \delta_c], v(t) = \left(\sum_{c' \in \text{CCo}(c)} v_{c'}^h(t - \delta_c + \Delta) + \sum_{s \in \text{CSy}(c)} v_s(h + t - \delta_c + \Delta) \right) \times \alpha_c.$

By extension, the family composed of the Δ -shifts of all the $v_c \in V$ is called the Δ -shift of V according to \mathcal{S} and it is noted $\Delta\text{-shift}(V, \mathcal{S})$.

Theorem 1. [Compartments dynamics] Given an initial dendritic state V^I of a neuron N and an input signal $\mathcal{S} = \{\omega_s\}_{s \in \text{Sy}(N)}$. There exists a unique dendritic state family $\{V^h\}_{h \in \mathbb{R}^+}$ such that:

- $V^0 = V^I;$
- for any Δ such that $0 \leq \Delta \leq \inf(\{\delta_c \mid c \in \text{Co}(N) \wedge \delta_c > 0\})$ and for any $h, V^{h+\Delta} = \Delta\text{-shift}(V^h, \mathcal{S})$.

Definition 10. [Dynamics of a neuron] Given a neuron N , a state $\eta^I = (V^I, e^I, p^I)$ and an input signal $\mathcal{S} = \{\omega_s\}_{s \in \text{Sy}(N)}$, the dynamics of N , according to \mathcal{S} with η^I as initial state, is the function $d_N : \mathbb{R}^+ \rightarrow \zeta_N$ defined by:

- $d_N(0) = \eta^I$
- $\forall h \in \mathbb{R}^+, d_N(h) = \eta^h = (V^h, e^h, p^h)$ where:
 - V^h is defined as in Theorem 1;
 - Consider beforehand the lipschitzian function $F(u) = \sum_{c \in \text{In}(\nabla)} v_c^u(0)$. According to Technical lemma 1, there exists a unique function P_F such that $P_F(e^I, p^I, 0) = p^I$ and $\forall u, \frac{dP_F(e^I, p^I, u)}{dh} = F(u) - \gamma \cdot P_F(e^I, p^I, u)$. If $P_F(e^I, p^I, u)$ is continuous on the interval $]0, h]$, then $e = e^I + h$. Otherwise, let u' be the greatest u such that $P_F(e^I, p^I, u)$ is discontinuous, then $e = h - u'$.
 - Considering the previous P_F function, $p = P_F(e^I, p^I, h)$.

4 SIMULATION OF THE HYBRID MODEL AND MODEL CHECKING

Our goal is to use our framework to prove particular properties of neurons. Our framework defines a hybrid process of signal integration *via* the dendritic tree, preserving linear equations. However, the integration at the soma inevitably induces a differential equation in order to preserve the essence of the biological functioning. This is unfortunately detrimental to computer-aided formal proving approaches. Therefore, the following step was to discretize time. Obviously, the smaller the time step is and the more accurate the result will be. But, one must also consider

the computational cost. The proper trade-off largely depends on the system we are interested in. When considering neuron spiking, events are usually assumed to be synchronous when happening in a given 1 to 5 milliseconds time window (Izhikevich, 2006; Brette, 2012; Grün et al., 1999). Therefore, our time step should be less than 1 millisecond. According to (Bower, 2003), 0.01 millisecond is an appropriate choice when looking at the shape of the action potential. Here, as we consider discrete spikes, we have chosen 0.1 millisecond as a reasonable *time step* (Δt).

4.1 Timing Discretization

For simulation and model checking purposes, all the temporal parameters have to be expressed in multiples of Δt .

Synapses. Usually, $\hat{\tau}$ (sometimes called time-to-peak) goes from one to tens of milliseconds and $\check{\tau}$ is most of the time greater (Williams and Stuart, 2002; Magee and Cook, 2000). This makes our time step appropriate, as a sufficiently large number of points will be considered in the trace of the signal (Figure 7).

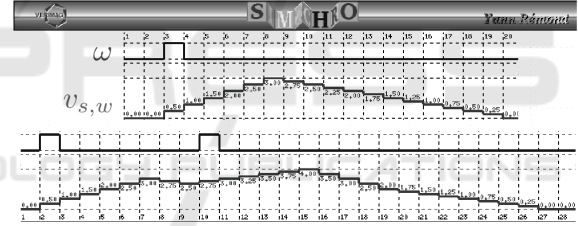


Figure 7: Simulation of a trace (v_s, ω) of an input signal (ω) on a synapse (s) with arbitrary parameters ($v = 3$, $\hat{\tau} = 6$ and $\check{\tau} = 12$). It is encoded in Lustre and simulated with Luciole. On the top is represented a trace in response to a single spike. On the bottom, the trace exhibits temporal summation.

Compartments. The delay for crossing a compartment (δ) being expressed in multiples of Δt , compartments smaller than $1\Delta t$ will be considered as null. This assumption may lead to kind of clusters of synapses, which are observed experimentally (Stuart et al., 2016; Gökçe et al., 2016).

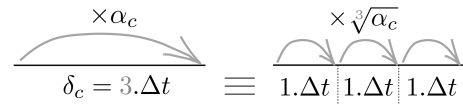


Figure 8: Division of a compartment into sub-compartments for proper discretization.

For each compartment, we define $n = \delta / \Delta t$ *sub-compartments* (noted subC, see Figure 8). Sub-compartments parameters are defined as follows:

$\delta_{subC} = 1\Delta t$ and $\alpha_{subC} = \sqrt[n]{\alpha}$ (where n is the number of sub-compartments in the original compartment and α is the attenuation of the original compartment). Given this representation, the dynamics is done by shifting all the sub-compartments at a time.

Soma. The major motivation for discretization is the time discretization at the soma. Basically, we chose to replace a differential equation with a difference to be solved at discrete time intervals (Δt). From Lemma 1, we have: $\frac{dP}{dt} = F(t) - \gamma.P(t)$. Once time is discretized, since P is piecewise linear, this equation is equivalent to $\frac{P(t+\Delta t) - P(t)}{\Delta t} = F(t) - \gamma.P(t)$. We thus have $P(t + \Delta t) - P(t) = (F(t) - \gamma.P(t)).\Delta t$. Therefore, we should use the following equation:
 $P(t + \Delta t) = F(t).\Delta t + P(t).(1 - \gamma.\Delta t)$.

Linearity properties (resulting from Definition 3) make this discretization exact. However, spikes times are approximated and this could lead to some error accumulation. Nevertheless, there is a limited risk of missing any spikes as the ARP is in the order of a millisecond, largely limiting the maximal frequency (Johnson, 2003).

4.2 Formal Proofs using Model Checking: a Simple Example

Based on our discretized model, we can use *model checking* in order to prove properties on neurons with dendrites in a computer-aided manner. Model checking allows one to automatically verify if a model satisfies a given property. We have chosen to encode our model in *Lustre* and using *Kind2* as model checker (with *z3* solver).

Lustre. Lustre is a synchronous programming language, working with flows. It benefits from a formal definition and it is particularly suited to reactive systems. A program in Lustre consists of *nodes*. A node computes outputs based on algebraic equations, accounting for input variables. All variables are typed. Local variables can be declared using the keyword *var*. The body of the node is composed of set of equations always true, surrounded by the keywords *let* and *tel*. For this reason, Lustre is a declarative language and not imperative. A node is declared as follows:

```
node nameOftheNode(input1: typeInput1; ...)
  returns(output1: typeOutput1; ...);
  var localVar1: typeVar1; ...;
  let
    Equations;
  tel
```

In Lustre, a variable does not carry a given value but a function of time, that is an infinite sequence of

values. As an example, to define a variable x , we should use the following syntax:
 $x = \text{initial value} \rightarrow \text{induction principle};$

The values carried by a variable are computed by a temporal recurrence expression which can depend on other variables. The *initial* value is the first value of the infinite sequence. It splits up the other values by the operator \rightarrow . Lustre has some elementary basic types (*bool*, *int*, *real*) and usual operators can be used on them ($+$, $-$, $*$, *etc.*; *and*, *or*, *not*; *if then else*). As an example, if a variable x is the infinite flow (x_1, x_2, \dots) and another variable y is the infinite flow (y_1, y_2, \dots) then, the variable $z = x + y$ is the infinite flow $(z_1 = x_1 + y_1, z_2 = x_2 + y_2, \dots)$.

Moreover there exists in Lustre an additional operator to deal with logical time: *pre()*. It acts as a memory by providing access to the previous value of a variable at a given time. For instance if the variable x is defined by $x = 0 \rightarrow \text{pre}(x) + 1$, the flow will be equal to 0 at time 0, equal to $0 + 1 = 1$ at time 1, equal to $1 + 1 = 2$ at time 2, and so on.

Any node can be simulated by a dedicated Lustre simulator called *luciole* (see Figure 7).

Kind2. There are several model checkers for Lustre. Kind2 relies on SMT (Satisfiability Modulo Theories) based k-induction and it proved to be efficient contrary to others model checkers such as *lesar*, *nbac*, *luke* and *rantanplan* (De Maria et al., 2016).

Kind2 is able to prove mathematical properties encoded as Lustre node: We write, in Lustre, the property as a boolean variable and Kind2 verifies if it is always true. As an example, to check if a variable x is equal to a variable y , meaning that at each time step the values of the two variables are the same, one can write the following node:

```
node property(x, y : int) returns (proof: bool);
  let
    proof = x = y;
  tel
```

Here, the output of the node *property* returns the value of *proof* which is true when $x = y$ and false otherwise. The property is thus satisfied if *proof* is always true whatever the values of x and y , at any time step.

A Simple Example.

As a first property to check, we have decided to compare the outputs of simple neurons for a given input and given initial states.

Let us consider the two neurons illustrated in Figure 9. Following Definition 10 and since both neurons have the same soma parameters, it is sufficient to compare the output of their dendritic forests. We have thus ignored the soma at first. We have encoded synapses and compartments in Lustre by defin-

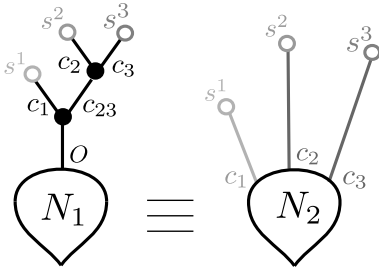


Figure 9: Example of two simple neurons. Their parameters are $\delta = 1$ and $\alpha = 0.5$ for all black compartments (in neuron N_1), $\delta = 2$ and $\alpha = 0.25$ for the light grey compartment (c_1 in neuron N_2), $\delta = 3$ and $\alpha = 0.125$ for dark gray compartments (c_2 and c_3 in neuron N_2). Synapses s_1 are defined by $v = 5$, $\hat{\tau} = 5$, $\check{\tau} = 15$, synapses s_2 are defined by $v = 3$, $\hat{\tau} = 6$, $\check{\tau} = 12$ and synapses s_3 are defined by $v = -5$, $\hat{\tau} = 5$, $\check{\tau} = 10$. N_1 and N_2 both have the same soma parameters.

ing nodes for each of them. Below, we show as an example, how a compartment can be defined for $\delta = 3 \cdot \Delta t$ (with $\alpha = 0.125$). Compartments with different parameters are encoded in the same way.

```
node comp3dt (I, init1, init2, init0 : real)
  returns (O : real);
  var c1, c2, alphaSubC : real;
  let
    alphaSubC = 0.5;
    c1 = init1 -> pre(I) * alphaSubC;
    c2 = init2 -> pre(c1) * alphaSubC;
    O = init0 -> pre(c2) * alphaSubC;
  tel
```

As shown in Figure 8, the compartment is divided into 3 sub-compartments with $\delta_{subC} = 1 \cdot \Delta t$ and $\alpha_{subC} = \sqrt[3]{0.125} = 0.5$. The node `comp3dt` takes as inputs real variables: the input (I) of the compartment (representing the signals coming from the contributor compartments or synapses) and the initial states ($init1$, $init2$, $init0$) of each sub-compartment. It then computes the output (O) of the whole compartment (with $init0$ as initial value). The variables ($c1$) and ($c2$) are the outputs of respectively the first and the second sub-compartments. The output of the first sub-compartment is computed from the value of the input I , one Δt before (using the operator `pre()`). Similarly, the output of the second sub-compartment is computed from the output of the first one, and so on.

To encode synapses, one node is required for each couple of parameters ($\hat{\tau}, \check{\tau}$). The node presented below encodes a simple excitatory synapse with $v = 1$, $\hat{\tau} = 2$ and $\check{\tau} = 4$.

```
node synapseE2_4 (omega : bool)
  returns (vs : real);
  var nu, hatTau, checkTau : real;
  o1, o2, o3, o4, o5 : bool;
  let
    nu = 1.0;
```

```
    hatTau = 2.0;
    checkTau = 4.0;
    o1 = false -> pre(omega);
    o2 = false -> pre(o1);
    o3 = false -> pre(o2);
    o4 = false -> pre(o3);
    o5 = false -> pre(o4);
    vs = 0.0 -> (if o1
      then nu/hatTau
      else 0.0)
      + (if o2
      then 2.0*nu/hatTau
      else 0.0)
      + (if o3
      then nu-nu/checkTau
      else 0.0)
      + (if o4
      then nu-2.0*nu/checkTau
      else 0.0)
      + (if o5
      then nu-3.0*nu/checkTau
      else 0.0);
  tel
```

The node `synapseE2_4` takes as input the boolean variable ω that represents the spikes sequence and computes the output vs that is the trace of the input signal ω on the synapse. The local variables nu , $hatTau$ and $checkTau$ are respectively the maximal potential variation triggered by a spike, the rise time and the descent delay. As shown in Figure 3, the contribution of a spike to the trace at a given time greatly depends on the time elapsed since the spike occurrence. The local boolean variable $o1$ is true if ω was true one time step before the current time, meaning that there was a spike at the previous time. Similarly, $o2$ is true if ω was true two time steps before the current time, meaning that there was a spike two times before, and so on. In this case, we have to look up to $\hat{\tau} + \check{\tau} - 1 = 5$ time steps back because beyond this time window a spike no longer influences the trace. In order to produce a temporal summation, the trace is computed from the contributions of all the preceding spikes. In the same way, we define nodes for inhibitory synapses called `synapseIx_y` where nu is a negative real number.

Once synapses and compartments are encoded as Lustre nodes, it is possible to define the entire dendritic forest for both neurons:

```
node neuron1(I1, I2, I3 : bool)
  returns (O : real);
  var S1, S2, S3, C1, C2, C3, C23,
    initC1, initC2, initC3, initC23,
    init0 : real;
  let
    initC1 = 0.0; initC2 = 0.0;
    initC3 = 0.0; initC23 = 0.0;
    init0 = 0.0;
    S1 = synapseE5_15(I1);
    S2 = synapseE6_12(I2);
```

```

        S3 = synapseI5_10(I3);
        C1 = compldt(S1, initC1);
        C2 = compldt(S2, initC2);
        C3 = compldt(S3, initC3);
        C23 = compldt(C2 + C3, initC23);
        O = compldt(C1 + C23, initO);
    tel

node neuron2(I1, I2, I3 : bool)
returns (O : real);
var S1, S2, S3, C1, C2, C3,
    initC11, initC12, initC21, initC22,
    initC23, initC31, initC32, initC33,
    initO : real;
let
    initC11 = 0.0; initC12 = 0.0;
    initC21 = 0.0; initC22 = 0.0;
    initC23 = 0.0; initC31 = 0.0;
    initC32 = 0.0; initC33 = 0.0;
    initO = 0.0;
    S1 = synapseE5_15(I1);
    S2 = synapseE6_12(I2);
    S3 = synapseI5_10(I3);
    C1 = comp2dt(S1, initC11, initC12);
    C2 = comp3dt(S2, initC21, initC22, initC23);
    C3 = comp3dt(S3, initC31, initC32, initC33);
    O = initO -> C1 + C2 + C3;
tel
    
```

Both nodes (`neuron1` and `neuron2`) compute a boolean output (`O`) from boolean inputs `I1`, `I2`, `I3` (representing sequences of spikes at synapses). As mentioned before, the two neurons have the same set of synapses (Figure 9). The real variables `S1`, `S2`, `S3` are the outputs of the nodes encoding respectively synapses s_1 , s_2 , s_3 with `I1`, `I2`, `I3` as inputs. They are thus used as inputs for compartments `compldt`, `comp2dt`, `comp3dt` whose outputs `C1`, `C2`, `C3`, `C23` are, in turn, used as inputs for other compartments. It allows ultimately to compute the output of the whole dendritic forest. For the sake of simplicity, compartment initial states were fixed to zero in both neurons. Under this condition and by considering constant inputs (always equal to true or false), we have proven that these two particular neurons (Figure 9) always produce the same outputs. All the possible inputs combinations ($2^3 = 8$) were verified. Below is the Lustre node encoding the property with `I1` and `I2` being always true and `I3` being always false:

```

node equivalence(gost : bool, epsilon: real)
returns (proof: bool);
var I1, I2, I3 : bool;
let
    I1 = true;
    I2 = true;
    I3 = false;
    proof = abs(neuron1(I1, I2, I3)
        - neuron2(I1, I2, I3)) < epsilon;
tel
    
```

Because neurons compute with real numbers, rounding errors in computation prevent to define proof as the simpler equality `neuron1(I1, I2, I3) = neuron2(I1, I2, I3)`; . In fact, with our example, this equality version the proof succeeds too: `neuron1` and `neuron2` make the same approximations.

We have also proven that the property is satisfied for other arbitrary inputs. As an example, we used `I1` being true on 1 *time step* in 50, `I2` being true on 1 *time step* in 10 and `I3` being true on 1 *time step* in 20.

For constant inputs, the model checker is remarkably efficient. For inputs with frequencies, we reach the limits of kind2 on a standard laptop, as the proof takes several hours.

Here, proofs have been entirely automatically handled by the model checker. Even though this example is simple, the ability of Kind2 to fully perform proofs without human guidance is encouraging.

5 CONCLUSION

We defined here the first hybrid *formal* model of neuron taking into account the morphology and its key role in neuronal computation. Our aim was to use formal methods from computer science to prove properties based on this framework. In order to make automatic proofs, we have used model checking. The main interest of this proof-based approach is the exploration of the whole space of possibilities inside a single proof. However, it requires models with discrete time. We thus proposed relevant abstractions of the neuron structure and dynamics with a subsequent time discretization.

Nevertheless, the number of parameters is still huge and it increases as we get closer to the biological reality. A “standard” neuron has thousands of synapses located on its dendrites making the system very complex.

Here, we successfully used model checking on a simple example. We proved that two particular neurons with different dendritic structures can have the same input/output function. This first result emphasises the crucial role of delays and attenuations rather than the importance of the precise dendrites morphology. It is partly a consequence of the hypotheses and choices we made. If we would like to incorporate some other biological properties (such as shunting) to our model, it would probably change this basic result (Häusser and Mel, 2003; Paulus and Rothwell, 2016; Gorski et al., 2017). But, even though our modelling relies on several simplifying assumptions,

it constitutes a first track to investigate the impact of the morphology on the neuron function, the first formal one.

As a direct continuation of this work, it would be interesting to make more general proofs and possibly with more complex and biologically relevant examples. The ultimate aim would be to automatically find constraints on parameters, such as observed delays provided by dendrites, for a model to satisfy a given behaviour. In another research direction, we think about building neuronal circuits. This would probably bring insights on how the neuronal structure could enable the emergence of complex behaviour at a larger scale.

REFERENCES

- Bianchi, S., Stimpson, C. D., Bauernfeind, A. L., Schapiro, S. J., Baze, W. B., McArthur, M. J., Bronson, E., Hopkins, W. D., Semendeferi, K., Jacobs, B., et al. (2012). Dendritic morphology of pyramidal neurons in the chimpanzee neocortex: regional specializations and comparison to humans. *Cerebral cortex*, 23(10):2429–2436.
- Börgers, C. (2017). Quadratic integrate-and-fire (qif) and theta neurons. In *An Introduction to Modeling Neuronal Dynamics*, pages 51–55. Springer.
- Bower, J.M., B. D. (2003). *The book of GENESIS: exploring realistic neural models with the General Neural Simulation System*. Internet Edition.
- Brette, R. (2003). *Modèles impulsifs de réseaux de neurones biologiques*. PhD thesis, Université Pierre et Marie Curie-Paris VI.
- Brette, R. (2012). Computing with neural synchrony. *PLoS computational biology*, 8(6):e1002561.
- Brette, R. and Gerstner, W. (2005). Adaptive exponential integrate-and-fire model as an effective description of neuronal activity. *Journal of neurophysiology*, 94(5):3637–3642.
- Brunel, N. and Van Rossum, M. C. (2007). Lapicques 1907 paper: from frogs to integrate-and-fire. *Biological cybernetics*, 97(5-6):337–339.
- Cook, E. P. and Johnston, D. (1997). Active dendrites reduce location-dependent variability of synaptic input trains. *Journal of neurophysiology*, 78(4):2116–2128.
- De Maria, E., Muzy, A., Gaffé, D., Ressouche, A., and Grammont, F. (2016). Verification of temporal properties of neuronal archetypes modeled as synchronous reactive systems. In *International Workshop on Hybrid Systems Biology*, pages 97–112. Springer.
- Gökçe, O., Bonhoeffer, T., and Scheuss, V. (2016). Clusters of synaptic inputs on dendrites of layer 5 pyramidal cells in mouse visual cortex. *eLife*, 5:e09222.
- Gorski, T., Veltz, R., Galtier, M., Fragnaud, H., Telenczuk, B., and Destexhe, A. (2017). Inverse correlation processing by neurons with active dendrites. *bioRxiv*.
- Grün, S., Diesmann, M., Grammont, F., Riehle, A., and Aertsen, A. (1999). Detecting unitary events without discretization of time. *Journal of neuroscience methods*, 94(1):67–79.
- Häusser, M. and Mel, B. (2003). Dendrites: bug or feature? *Current opinion in neurobiology*, 13(3):372–383.
- Häusser, M., Spruston, N., and Stuart, G. J. (2000). Diversity and dynamics of dendritic signaling. *Science*, 290(5492):739–744.
- Hodgkin, A. L. and Huxley, A. F. (1952). A quantitative description of membrane current and its application to conduction and excitation in nerve. *The Journal of physiology*, 117(4):500–544.
- Hu, H. and Vervaeke, K. (2017). Synaptic integration in cortical inhibitory neuron dendrites. *Neuroscience*.
- Izhikevich, E. M. (2006). Polychronization: computation with spikes. *Neural computation*, 18(2):245–282.
- Johnson, L. R. (2003). *Essential medical physiology*. Academic Press.
- Johnston, D. and Narayanan, R. (2008). Active dendrites: colorful wings of the mysterious butterflies. *Trends in neurosciences*, 31(6):309–316.
- Koch, C. (2004). *Biophysics of computation: information processing in single neurons*. Oxford university press.
- Lapicque, L. (1907). Recherches quantitatives sur l’excitation électrique des nerfs traitée comme polarisation. *J. Physiol. Pathol. Gen.*, 9:620–635.
- Maass, W. (1996). Lower bounds for the computational power of networks of spiking neurons. *Neural computation*, 8(1):1–40.
- Maass, W. (1999). Computing with spiking neurons. *Pulsed neural networks*, 85.
- Magee, J. C. and Cook, E. P. (2000). Somatic epsp amplitude is independent of synapse location in hippocampal pyramidal neurons. *Nature neuroscience*, 3(9):895.
- Manita, S., Miyakawa, H., Kitamura, K., and Murayama, M. (2017). Dendritic spikes in sensory perception. *Frontiers in cellular neuroscience*, 11.
- McCulloch, W. S. and Pitts, W. (1943). A logical calculus of the ideas immanent in nervous activity. *The bulletin of mathematical biophysics*, 5(4):115–133.
- Mel, B. W. (1994). Information processing in dendritic trees. *Neural computation*, 6(6):1031–1085.
- Mohan, H., Verhoog, M. B., Doreswamy, K. K., Eyal, G., Aardse, R., Lodder, B. N., Goriounova, N. A., Asamoah, B., Brakspear, A. C., Groot, C., et al. (2015). Dendritic and axonal architecture of individual pyramidal neurons across layers of adult human neocortex. *Cerebral Cortex*, 25(12):4839–4853.
- Paulus, W. and Rothwell, J. C. (2016). Membrane resistance and shunting inhibition: where biophysics meets state-dependent human neurophysiology. *The Journal of physiology*, 594(10):2719–2728.
- Popper, K. R. (1963). *Conjectures and refutations: the growth of scientific knowledge*.
- Rall, W. (1959). Branching dendritic trees and motoneuron membrane resistivity. *Experimental neurology*, 1(5):491–527.

- Rall, W. (1962). Theory of physiological properties of dendrites. *Annals of the New York Academy of Sciences*, 96(1):1071–1092.
- Rall, W. (1967). Distinguishing theoretical synaptic potentials computed for different soma-dendritic distributions of synaptic input. *Journal of neurophysiology*, 30(5):1138–1168.
- Rall, W. (2011). Core conductor theory and cable properties of neurons. *Comprehensive physiology*.
- Remme, M. W., Lengyel, M., and Gutkin, B. S. (2010). Democracy-independence trade-off in oscillating dendrites and its implications for grid cells. *Neuron*, 66(3):429–437.
- Stuart, G., Spruston, N., and Häusser, M. (2016). *Dendrites*. Oxford University Press.
- Stuart, G. J. and Spruston, N. (2015). Dendritic integration: 60 years of progress. *Nature neuroscience*, 18(12):1713–1721.
- Sun, Q., Srinivas, K. V., Sotayo, A., and Siegelbaum, S. A. (2014). Dendritic na⁺ spikes enable cortical input to drive action potential output from hippocampal ca2 pyramidal neurons. *Elife*, 3:e04551.
- Williams, S. R. and Stuart, G. J. (2002). Dependence of epsp efficacy on synapse location in neocortical pyramidal neurons. *Science*, 295(5561):1907–1910.

